Sensors and Actuators B 260 (2018) 198–203

Contents lists available at ScienceDirect

Sensors and Actuators B: Chemical

journal homepage: www.elsevier.com/locate/snb

Q-factor enhancement of piezoelectric MEMS resonators in liquids with active feedback

M. Fischeneder*, M. Kucera, F. Hofbauer, G. Pfusterschmid, M. Schneider, U. Schmid

Institute of Sensor and Actuator Systems, TU Wien, Vienna, 1040, Austria

ARTICLE INFO

Article history:
Received 19 September 2017
Received in revised form
20 December 2017
Accepted 1 January 2018
Available online 2 January 2018

Keywords:
Quality factor enhancement
Analogue feedback
Liquid media
MEMS
Q-factor

ABSTRACT

For a precise determination of the density and viscosity of liquids with MEMS resonators, a high Q-factor is of utmost importance. In such environments, in-plane resonant modes offer a lower damping compared to out-of-plane modes, thus allowing to quantify the increase in Q-factor with and without electrical feedback directly. To stimulate an in-plane oscillation, a sputter deposited aluminum nitride layer on a silicon cantilever is driven by a Lock-In amplifier which is adjusted by the feedback signal originating from the piezoelectric thin film. The exposure to selected liquids, ranging from ethanol to N35 with a dynamic viscosity from 1.2 mPa s up to 73.2 mPa s, features at room temperature intrinsic Q-factors of about 40 and 8, respectively. With a carefully designed amplification circuit, the Q-factors are increased by a factor of 1.4 up to 9.3, which represents Q-factors of 374–12, demonstrating the high potential especially at low viscous liquids.

1. Introduction

Silicon based micro electro-mechanical systems (MEMS) sensors and actuators made an enormous progress in the last few decades. A large variety of sensor elements for different applications such as the detection of chemical [1–3] or physical quantities [4–7] were developed and are commercially available nowadays. Independent of their field of application, however, in most cases either membranes or cantilevers are used as core components in MEMS device architectures. A substantial increase in sensitivity is realised when MEMS devices are operated in resonance, applying either electro-magnetic, capacitive or piezoelectric elements for excitation [8].

When the latter transducer principle is targeted, the active element may consist of an aluminum nitride layer (AlN), which is sputter deposited on silicon (Si) [9–11]. Compared to lead zirconate titanate (PZT), AlN is often preferred as functional material despite its moderate piezoelectric coefficients [9,12], as it is compatible with standard complementary metal oxide semiconductor (CMOS) microfabrication processes [13] and it offers high temperature stability up to about 1000 °C [14]. Most promising application scenarios for cantilever or membrane-type micro machined AlN devices are as density and viscosity sensors of liquids [15,16], as high frequency filters [17,18], as MEMS scanning mirrors [19] or as vibrational energy harvesters [20].

When operated in liquids, however, the intrinsic Q-factor of a MEMS resonator is strongly reduced due to high damping, especially for any out-of-plane cantilever oscillation. Therefore, in-plane modes are preferred as the surface fraction of the resonator being perpendicular to its oscillation direction is minimized. Using this approach it is possible to evaluate liquids with a dynamic viscosity from 1.2 mPa s to 73.16 mPa s (i.e. ethanol, isopropanol and reference standards D5, N10, S20 and N35) with moderate Q-factors [15]. To increase the sensitivity of the MEMS resonators higher Q-factors of this mode are targeted.

One of the key parameter of resonantly excited cantilevers is the intrinsic Q-factor which corresponds to open-loop operation. To increase the electrical output from the piezoelectric element in air, the intrinsic Q-factor of the resonator is increased to an effective Q-factor by amplifying the original output signal and feed it back to the cantilever via a carefully designed supply circuit in closed-loop-operation [15,21]. Basically, the resonance peak height is low compared to the parasitic base signal without compensation. An additional compensation structure helps to eliminate this parasitic effect. To demonstrate the advantage of this approach the cantilever-type MEMS resonator is exposed to different fluids and finally, both the intrinsic and the effective Q-factors are measured and discussed.

* Corresponding author.
E-mail address: martin.fischeneder@tuwien.ac.at (M. Fischeneder).

https://doi.org/10.1016/j.snb.2018.01.001
0925-4005/

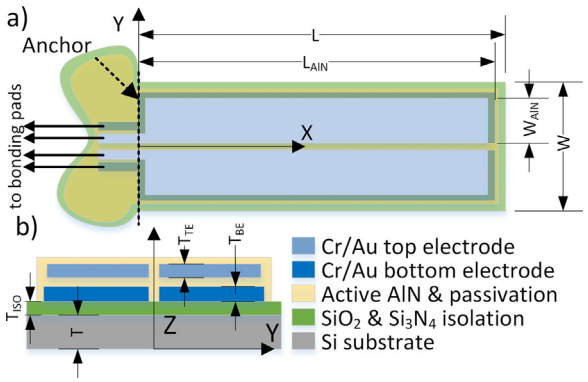

Fig. 1. Schematic of the cantilever. (a) The top view includes the two pairs of top- and bottom electrodes and (b) the cross-section views the layer stack.

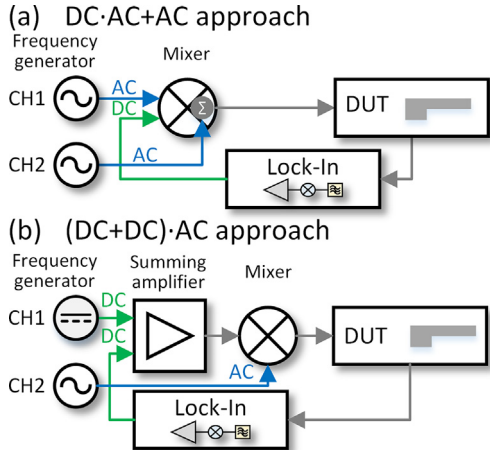

Fig. 2. Schematic of electric circuit of Q-control. (a) AC·DC + AC approach and (b) (DC + DC)·AC approach.

2. Experimental details

The experiments are performed with a cantilever based on a SOI wafer with a device layer thickness of $T = 20\,\mu m$, having a length of $L = 2017\,\mu m$ and width of $W = 1272\,\mu m$ (Fig. 1). The wafer is coated with a low stress oxynitride layer which electrically insulates the Chromium (Cr) and Gold (Au) bottom electrodes. The active piezoelectric layer is sputter-deposited and subsequently patterned, whereas a bi-layer of Cr and Au serves as top electrode. In Ref. [15] details of the fabrication process are presented. Finally, the cantilevers are ready to be diced, released and mounted in a standard DIP24 package (Minitron).

2.1. Q–control setup

To realise an active Q-factor enhancement of cantilever-type piezoelectric MEMS resonators, two basic approaches are evaluated as shown in Fig. 2. The circuit design differs in the implementation of the mixing stage of AC and DC voltage components. The DC·AC + AC approach (see Fig. 2(a)) shifts the feedback signal (DC) of the Lock-In amplifier with CH1 (AC) of the frequency generator from baseband to passband and is used as the sinusoidal carrier signal. Next, the initial driving voltage of CH2 of the frequency generator is added as an additional AC signal component at the mixer. But, there is a phase lag at this stage caused by non-linearity of the mixer which cannot be compensated completely. Instead of this type of Q-control an analogue Q-control approach (DC + DC)·AC is implemented (see Fig. 2(b)) for active Q-control where the adding stage of the mixer is not used. Despite the increased amount of electronic elements this approach prevents any phase shifting by adjusting the demodulation phase of the Lock-In amplifier [16].

Basically, the Q-control with the (DC + DC)·AC approach avoids variable time lags of the mixing step and allows an easier phase lag compensation. A schematic overview reveals the separation of the amplifier which sums up the DC-signals (V_{in} and V_{fbG}), and of the mixer stage which shifts the signal from baseband to passband, as presented in Fig. 3. A detailed discussion of the phase lag is given in the next chapter.

A LabVIEW program (Control software) controls and reads out the Agilent 33522A frequency generator and the Zürich Instruments HF2LI Lock-In amplifier. The initial stimulus is generated by the use of a DC value $V_{in} = -10\,mV$ (CH1) and a sinusoidal carrier voltage $V_{AC} = 3\,V$ RMS (CH2). This results in an effective amplitude of $V_c = 8\,mV$, which is applied to the MEMS resonator far off the resonance frequency. The Lock-In amplifier extracts the voltage converted current signal (I/U converter) from the carrier-wave and filters it with an internal low-pass filter at a cut-off frequency of $f_{-3db} = 10\,Hz$.

The dominating time constant of this Q-control setup is given by the internal low-pass filter of the Lock-In amplifier. The Lock-In amplifier supports an auxiliary output with 16-bit digital/analogue converter (DAC) with 1 MSample/s and ±10 V with 200 kHz analogue bandwidth. This high-speed auxiliary output generates the feedback signal (V_{fbG}) and is summed up with CH1 of the function generator at the amplifier. The CH1 delivers the initial DC value of the stimulus V_{in} and CH2 is used to synchronise the Lock-In amplifier with the sinusoidal carrier voltage V_{AC}, which is internally connected to the trigger output. This synchronisation determines the real and imaginary part of the resonator response characteristics.

For summing up the signals, a precision operational amplifier OPA277 is implemented, which features an ultra-low offset voltage of about 10 µV. The output of the summing amplifier ($V_{in} + V_{fbG}$) is multiplied at the mixer AD734 with the sinusoidal carrier signal $V_{AC} = V\sin(\omega t + \phi_0)$. A THS4151 from Texas Instruments is used for the fully differential amplifier stage (driver stage). This device offers an operation up to ±15 V dual power supply and a high unity gain bandwidth of 150 MHz combined with a high slew rate of 650 V/µs. For the I–V converter a low noise high-speed precision operational amplifier LT1037 is implemented. An optical photograph of the custom-made electronic circuit realised on a double-sided PCB is shown in Fig. 4.

2.2. Phase compensation procedure

The analogue approach requires a low phase lag between the driving AC voltage applied to the MEMS resonator and the synchronisation signal provided by the function generator. Any additional phase lag has to be taken into account and compensated in order to extract the real part V_G from the output voltage. The trigger output of CH2 of the function generator is connected to the digital IO (DIO) of the HF2LI and used as a synchronisation channel. Thereby, the phase shift ϕ_0 between frequency generator and V_G was determined in the frequency range from 100 kHz to 1 MHz. By tuning the demodulator of the Lock-In amplifier with the LabView control software, a stepwise compensation of the phase is realised, which is shown in Fig. 5. From Fig. 5(a) a linear phase shift is identified as the dominant component of ϕ_0 which is compensated with an equivalent time constant of $\tau_0 = 75\,ns$ (see Fig. 5(b), curve 1). The internal range switch of the function generator at 250,500 and 975 kHz is compensated as illustrated in Fig. 5(b), curve 2 and this phase shift was piecewise linear approximated, as illustrated in Fig. 5(b), curve 3. This effort leads to a phase lag of <0.1° in a frequency range of 100 kHz to 1 MHz (see Fig. 5(b), curve 4).